

Rapid Communications

Rapid Communications are intended for the accelerated publication of important new results and are therefore given priority treatment both in the editorial office and in production. A Rapid Communication in Physical Review B should be no longer than four printed pages and must be accompanied by an abstract. Page proofs are sent to authors.

Phase diagram for mercury up to 67 GPa and 500 K

Olaf Schulte and Wilfried B. Holzapfel

Universität Gesamthochschule Paderborn, 33095 Paderborn, Germany

(Received 23 July 1993; revised manuscript received 7 September 1993)

The pressure-temperature phase diagram for mercury is determined using energy-dispersive x-ray diffraction and a diamond anvil cell. In addition to the well-known structures of Hg, one new modification was found to be stable in the present experimental region. An orthorhombic lattice with four atoms in the unit cell represents all the experimental data for this new phase. The locations of the phase boundaries between the different phases α - β - γ - δ are determined for the extended p - T region. Furthermore, the parameters of the equations of state of the different phases are evaluated.

The phase diagram of mercury up to 7 GPa is well known¹ and the melting curve has often been used as a pressure standard. At ambient temperature, mercury transforms at 3.7 GPa from the low-pressure rhombohedral structure (α -Hg, space group $R\bar{3}m$, $N=2$ equivalent atoms in the unit cell) to a body-centered-tetragonal (bct) structure (β -Hg, $I4/mmm$, $N=2$). New features were discovered at first at 12(2) GPa and further more at 37(3) GPa when the pressure range was extended to 39 GPa.² The patterns above 37 GPa were indexed unambiguously by a hexagonal closed-packed structure (δ -Hg, $P6_3/mmc$, $N=2$) which is designated often also as hcp, however, the value for $c/a=1.76$ deviates significantly from the ideal value of 1.663. This structure was also predicted theoretically.³ The patterns for the intermediate region between 12 and 37 GPa at ambient temperature were indexed in this previous study as resulting from a mixture of the three phases α , β , and δ .² The present study, using synchrotron radiation with higher resolution in an extended pressure range up to 67 GPa, gave, however, clear evidence for additional lines in the intermediate region which are not compatible with the previous indexing for this region, but could be indexed to a simple orthorhombic structure.

Diffraction patterns of Hg were obtained by the energy-dispersive x-ray-diffraction (EDXD) technique using synchrotron radiation at the station F3 at HASYLAB, DESY. The experimental setup has been described in detail previously.⁴ On the other hand, some data were also obtained by more conventional techniques using a laboratory x-ray tube with the conical slit arrangement and a fourfold detector system.⁵ Both experimental techniques have a better resolution (roughly by a factor of 2) than the previously used large area detector system.⁶ High pressure was generated with a gasketed diamond anvil cell^{7,8} (DAC) which includes also internal heaters to reach temperatures up to 500 K at the sample

position.⁹ For the low-temperature measurements, the DAC was clamped to a liquid-nitrogen bath cryostat, which allows one to cool the sample to 150 K.⁴ The temperature was measured with a thermocouple fixed to the bottom of one diamond and the pressure was determined by the ruby luminescence technique¹⁰ with the nonlinear pressure scale¹¹ using also the common temperature correction.^{12,13} Liquid nitrogen as well as mineral oil were used as pressure transmitting media inside the sample hole. Either solidified mercury was meshed and loaded into the sample chamber under a nitrogen atmosphere or very small droplets were filled in at ambient conditions, respectively.

Three structural phase transitions are observed in the present pressure range up to 67 GPa. Beside the well-known transition at 3.7 GPa from α -Hg (rhombohedral, $R\bar{3}m$, $N=2$) to β -Hg (bct, $I4/mmm$, $N=2$), two additional transitions could be discerned clearly in the present study. The first transition occurs at 12(2) GPa (at room temperature). This structure (γ -Hg) is stable to 37(3) GPa. At 37(3) GPa a second transition to δ -Hg (hcp) occurs and this structure is preserved up to the highest pressure. Typical spectra of mercury taken with synchrotron radiation for the different structures are shown in Fig. 1. The indexing of the pattern for 9.2 GPa corresponds to a bct lattice. At 46.8 and 61.8 GPa the hcp indexing is shown. The pattern at 19.8 GPa is typical for the new phase. It is indexed by a simple orthorhombic lattice with four atoms in the unit cell. In contrast to the earlier suggestions, where this region was considered to show bct, rhombohedral, and hcp structures, the present measurements with higher resolution reveal clearly now some additional lines which do not fit to bct or hcp structures. These new lines are marked in Table I by an asterisk. The orthorhombic indexing, however, represents all the observed lines. Table I gives a comparison of observed and calculated lattice spacings for a pat-

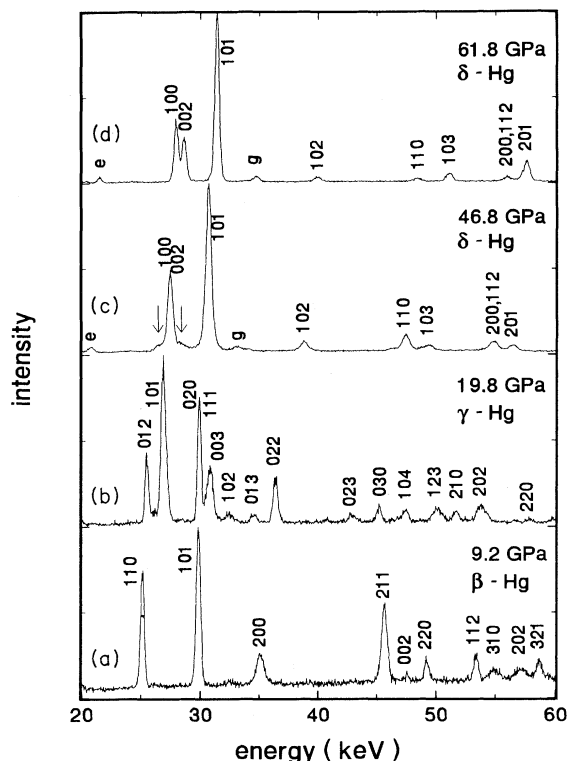


FIG. 1. Diffraction patterns of Hg at room temperature and under different pressures. (a) β -Hg (bct), (b) γ -Hg (orthorhombic), (c) and (d) δ -Hg (hcp). *g* denotes diffraction lines from the gasket, *e* indicates escape peaks from the Ge detector. The arrows mark diffraction peaks of rest from the orthorhombic phase.

tern taken at 19.8 GPa which is well in the middle of the stability range of the new phase. The observed intensities of the diffraction lines are also given in Table I as well as the calculated lattice spacings for the (former assumed) bct, rhombohedral, and hcp lattices. A space-group analysis with these reflections of the orthorhombic structure was not successful, because no characteristic extinc-

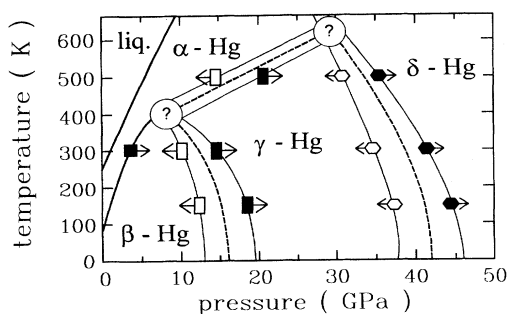


FIG. 2. Phase diagram of mercury. Closed and open symbols represent forward and backward transitions, respectively. The shaded areas show the regions of hysteresis and the question marks indicate roughly the locations of the triple points.

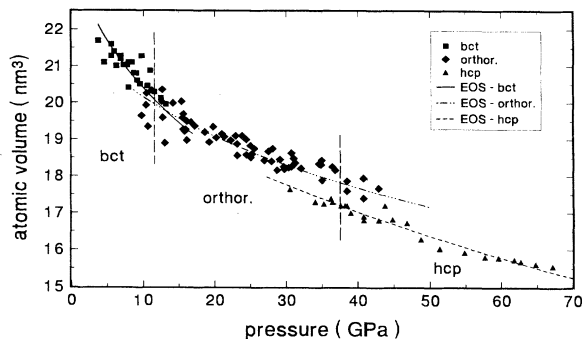


FIG. 3. Pressure-volume data of mercury at room temperature. The curves represent the EOS obtained by the form given in the text for the different phases.

tions were found due to the large number of overlapping lines. Further studies are necessary to find out the space group, for instance, at smaller diffraction angles to spread out the pattern and to include possible diffraction lines with lower indices.

With the measurements at lower and higher temperatures, Fig. 2 represents the present results on the various phase transition lines. Thick solid lines show the previous boundaries,¹ dashed lines represent the results of the present study. The equilibrium transition pressures are taken as midpoints of the hysteresis loops. A rough estimation of the slope of the boundary lines, dp/dT , neglecting the curvature leads to values of -0.025 GPa/K for the β - γ phase boundary, -0.0244 GPa/K for the γ - δ , and $0.13(5)$ GPa/K for the α - γ boundary line with a much larger uncertainty than for the other boundaries, since the locations of the triple points α - β - γ and α - γ - δ are still rather uncertain due to a lack of sufficient data along the α - γ transition line.

For further evaluation of the present results a numerical representation of the equation of state (EOS) data for the different phases can be desirable (see Fig. 3). While a detailed discussion of these data requires some special considerations about the most appropriate EOS form,^{14,15} which will be given for this case elsewhere,¹⁶ a numerical representation can be given already here. This evaluation is strictly limited to the range of the experimental data as indicated for the three phases of Hg in the last column of Table II. A Murnaghan-type EOS is used with the form

$$V = V_r [1 + (p - p_r) K'_r / K_r]^{K'_r},$$

which includes in addition to the original form¹⁷ a reference pressure p_r . Here, p_r is selected (almost arbitrarily) in the center of the stability range or experimental range of the corresponding p - V data to minimize the correlations in the three fit parameters V_r , K_r , and K'_r , which represent, respectively, the atomic volume, the bulk modulus, and its pressure derivative at the reference pressure p_r . The results of the least-squares fitting for the Murnaghan-type EOS are given in Table II. Due to the implicit assumption of the Murnaghan EOS that K'_r is constant, a reasonable approximation for $K(p)$ is given by

TABLE I. Comparison of observed lattice spacings and intensities at 19.8 GPa with calculated d values for an orthorhombic lattice ($a = 269.1$ pm, $b = 445.7$ pm, $c = 645.4$ pm) and for the bct, hcp, and rhombohedral lattices, respectively. Observed lines marked with an asterisk do not fit to a hypothetical mixed phase pattern.

hkl	d_{obs} (pm)	$d_{\text{calc}}^{\text{orthor}}$ (pm)	I_{obs} (%)	$d_{\text{calc}}^{\text{bct}}$ (pm)	$d_{\text{calc}}^{\text{hcp}}$ (pm)	$d_{\text{calc}}^{\text{rhomboh}}$ (pm)
001		645.4				
010		445.7				
011		366.8				
002		322.7				
100		269.1				
012	*	262.1	41			
				259.5(110)		
					252.1(002)	
101	248.5	248.4	100		247.9(100)	247.7(101)
110		230.4				
020	223.3	222.9	77	223.6(101)	222.5(101)	
111	*	217.0	31			
003	215.7	215.1	7			
						213.8(003)
021		210.7				
102	205.7	206.8	7			205.9(102)
013	*	193.6	5			
112		187.5				
022	183.5	183.4	27	183.5(200)		
					176.8(102)	
120		171.6				
103		168.0				
121		165.9				
004		161.4				
113	155.6	157.2				
023	155.6	154.8	5			155.0(110)
014		151.7				
122		151.5				
030	*	147.8	10			
031	142.0	144.7	3	141.9(211)	143.1(110)	
104	140.7	138.4	6	141.0(002)	139.2(103)	
						137.7(104)
032		135.0				
200	*	133.2				
123	*	133.2	7			
114	*	133.2				
201		131.7				131.4(201)
024	129.1	130.7				
130	129.1	130.1	7	129.8(220)		
005	129.1	129.1				
210	129.1	128.8				
131		127.5				
211		126.3			126.2(004)	
202	124.1	124.2			124.5(112)	125.5(113)
015	124.1	124.0	10	123.9(112)	124.0(200)	123.8(202)
033	121.8	122.3				
132	121.8	120.6	1		120.4(201)	
212		119.6				
124		117.6				
105	115.4	116.4		116.1(310)		115.7(105)
220	115.4	115.1	3			
203	115.4	114.1				
221		113.4				
115	111.7	112.6		112.3(301)	112.5(104)	
025	111.7	111.7		111.8(202)		
040	111.7	111.4				
133	111.7	111.3	3		111.2(202)	

TABLE II. Parameters for the representation of the p - V data at room temperature in the different phases by the use of a Murnaghan equation.

	p_r (GPa)	V_r (nm ³)	K_r (GPa)	K'_r	Range (GPa)
bct	8	0.020 76(5)	81(23)	2(1)	4–12
Orthor.	27	0.018 68(4)	267(17)	8.5(4)	10–43
hcp	40	0.016 15(5)	271(19)	4.2(3)	30–67

$$K(p) = K_r + (p - p_r)K'_r$$

just for the limited experimental regions. An extrapolation of these relations to $p = 0$ GPa to determine K_0 and

K'_0 seems mostly not reasonable due to the large uncertainties in K'_r and requires EOS forms with more physical input.^{14–16}

Finally, it should be noted that the new results on the phase diagram of mercury are fully compatible with the theoretical study,³ however, the new orthorhombic structure was not included in these theoretical considerations and may thus stimulate further theoretical studies to fully describe the phase diagram of Hg also from a theoretical point of view.

The authors thank the German Ministry of Science and Technology (BMFT) for financial support under Contract No. 05 440 AXI4.

- ¹W. Klement, A. Jayaraman, and G. C. Kennedy, *Phys. Rev.* **131**, 1 (1963).
²O. Schulte and W. B. Holzapfel, *Phys. Lett. A* **131**, 38 (1988).
³J. A. Moriarty, *Phys. Lett. A* **131**, 41 (1988).
⁴W. A. Grosshans, E. F. Düsing, and W. B. Holzapfel, *High Temp. High Press.* **16**, 539 (1984).
⁵H. W. Neuling, O. Schulte, T. Krüger, and W. B. Holzapfel, *Meas. Sci. Technol.* **3**, 170 (1992).
⁶W. B. Holzapfel and W. May, in *High Pressure Research Geophysics*, edited by S. Akimoto and H. M. Manghani, *Advances in Earth and Planetary Sciences Vol. 12* (Kluwer Academic, Dordrecht, 1982), p. 73.
⁷K. Syassen and W. B. Holzapfel, *Europhys. Conf. Abstr.* **1A**, 75 (1975).
⁸W. B. Holzapfel, in *High Pressure Chemistry*, edited by H. Kelm (Reidel, Boston, 1978), p. 177.
⁹B. Merkau and W. B. Holzapfel, *Physica B+C* **139/140**, 251 (1986).
¹⁰G. J. Piermarini, S. Block, J. D. Barnett, and R. A. Forman, *J. Appl. Phys.* **46**, 2774 (1975).
¹¹H. K. Mao, P. M. Bell, J. W. Shaner, and D. J. Steinberg, *J. Appl. Phys.* **49**, 3276 (1977).
¹²R. A. Noack and W. B. Holzapfel, in *High Pressure Science and Technology*, edited by K. D. Timmerhaus and M. S. Barber (Plenum, New York, 1979), Vol. 1, p. 748.
¹³R. G. Munro, G. J. Piermarini, S. Block, and W. B. Holzapfel, *J. Appl. Phys.* **67**, 2 (1985).
¹⁴W. B. Holzapfel, *Molecular Systems Under High Pressure*, edited by R. Pucci and G. Piccitto (Elsevier, Amsterdam, 1991), p. 61.
¹⁵W. B. Holzapfel, *Europhys. Lett.* **16**, 539 (1991).
¹⁶O. Schulte, Ph.D. thesis, Universität Gesamthochschule Paderborn, 1993.
¹⁷F. D. Murnaghan, *Finite Deformation of an Elastic Solid* (Wiley, New York, 1951).